Magneto-plasmon modes in a terahertz-driven electron gas

1999 J. Phys.: Condens. Matter 11 L355

(http://iopscience.iop.org/0953-8984/11/30/101)

J. Phys.: Condens. Matter **11** (1999) L355–L361. Printed in the UK PII: S0953-8984(99)04283-6

LETTER TO THE EDITOR

Magneto-plasmon modes in a terahertz-driven electron gas

W Xu

Department of Engineering Physics, Institute for Superconducting and Electronic Materials, University of Wollongong, Wollongong, NSW 2522, Australia

E-mail: wxu@wumpus.its.uow.edu.au

Received 13 May 1999

Abstract. A theoretical study of the plasmon modes is presented for an ideal three-dimensional electron gas (3DEG) subjected simultaneously to linearly polarized intense laser fields and to quantizing magnetic fields. The dependence of the magneto-plasmon excitation on the frequency and intensity of the laser field and on the magnetic field in a GaAs-based 3DEG system is investigated in detail and the results are pertinent to the application of terahertz free-electron laser sources developed very recently.

The recent application of far-infrared (FIR) or terahertz (10^{12} Hz or THz) free-electron laser (FEL) radiation to scientific investigation into Si- and GaAs-based systems [1, 2] has opened up a new field of research in condensed matter physics and semiconductor optoelectronics. For semiconductor materials such as Si and GaAs, *terahertz* is a very interesting frequency bandwidth lying between 'optical' and 'electrical' phenomena, because in these materials the rate of electronic transitions via scattering with impurities and phonons [3] and via fast electron processes [4] is in the order of 10^{12} s^{-1}. THz radiation will modify strongly the processes of momentum and energy relaxation for excited electrons in the system. Moreover, a very recently achieved experimental set-up [5] has made it possible to perform measurements of a semiconductor device under THz FEL radiation, in the presence of strong static magnetic fields. When an electron gas, as realized, e.g. in a bulk semiconductor, is subjected simultaneously to intense THz laser fields and to quantizing magnetic fields, we enter a regime of different competing energies. In this case, the Fermi energy, the cyclotron energy and the plasmon energy of the electronic system can be comparable to the THz photon energy and to that of the radiation field. As a result, the THz laser field can couple strongly to the electronic system and can affect significantly the electronic structure of the device. Hence, one expects that in the presence of intense THz radiation the collective excitations, such as magneto-plasmons, will differ significantly from those [6] observed in the absence of the laser field. In this letter, I examine theoretically how a linearly polarized THz radiation affects the spectrum of magneto-plasmon in a semiconductor-based electron gas system.

In the present study, I consider the situation where a static magnetic field $\boldsymbol{B}$ is applied along the z-axis of an ideal three-dimensional electron gas (3DEG) and a laser field $\boldsymbol{A}(t)$ is linearly polarized parallel to $\boldsymbol{B}$. In this case, the magnetic potential does not couple directly to the electromagnetic (EM) potential and, therefore, the effect of cyclotron resonance is not present. Moreover, in this configuration the time-dependent single-electron Schrödinger equation in the presence of $\boldsymbol{A}(t)$ and $\boldsymbol{B}$ fields can be solved exactly [7]. Thus, we can first investigate the electronic properties in the $(\boldsymbol{Q}, t)$ representation (i.e. in the momentum–time space) using a time-dependent many-body theory [8].

0953-8984/99/300355+07$30.00

(1) From the time-dependent electron wavefunction obtained from the solution of the Schrödinger equation, one can determine the retarded $G^+(N, k_z; t > t')$ and advanced $G^-(N, k_z; t > t')$ Green functions for electrons [7], where N is the index for the Nth Landau level (LL) and k_z is the electron wavevector along the z-direction along which the EM field is polarized.

(2) From these Green functions, we can derive the electron density–density correlation function (or pair bubble) $\Pi(\boldsymbol{Q}; t > t')$ for a Fermi system at finite temperatures [9], where $\boldsymbol{Q} = (\boldsymbol{q}, q_z) = (q_x, q_y, q_z)$ is the change of the electron wavevector.

(3) Applying these results to the random-phase approximation (RPA) diagrams for the effective electron–electron (e–e) interaction, we obtain the inverse RPA dielectric function $1/\epsilon(\boldsymbol{Q}; t > t')$ [9]. After first Fourier analysing $G^+(N, k_z; t > t')$ and $1/\epsilon(\boldsymbol{Q}; t > t')$ according to the relative coordinates $\tau = t - t'$ then averaging the initial time t' in these quantities over a period of the radiation field, we can obtain the electron density of states (DOS) [7] and the inverse RPA dielectric function [9] in the $(\boldsymbol{Q}; \Omega)$ representation (i.e. in the momentum–spectrum space), respectively, as

$$D_N(E) = \frac{g_s a}{4\pi^2 l^2} \sum_{m=-\infty}^{\infty} \frac{\Theta(\mathcal{E}_{Nm})}{\mathcal{E}_{Nm}^{1/2}} F_m^2(a\mathcal{E}_{Nm}^{1/2}) \tag{1}$$

and

$$\frac{1}{\epsilon(\boldsymbol{Q}, \Omega)} = \sum_{m=-\infty}^{\infty} \frac{J_m^2(r_0 q_z)}{1 - V(Q)\Pi_0(\boldsymbol{Q}, \Omega + m\omega)}. \tag{2}$$

Here, ω is the frequency of the radiation field, F_0 is the strength of the radiation electric field, and the index m refers to different optical processes. $m > 0$ ($m < 0$) corresponds to m-photon absorption (emission) and $m = 0$ to a channel of elastic photon scattering. In equation (1), $g_s = 2$ accounts for the spin degeneracy, $a = (2m^*/\hbar^2)^{1/2}$ with m^* being the effective electron mass, $l = (\hbar/eB)^{1/2}$ is the radius of the ground cyclotron orbit, $\mathcal{E}_{Nm} = E - E_N - E_{em} - m\hbar\omega$, $E_N = (N + 1/2)\hbar\omega_c$ is the energy of the Nth LL with ω_c being the cyclotron frequency, and $E_{em} = 2\gamma\hbar\omega$ is the energy of the radiation field (induced by the dynamical Franz–Keldysh effect [10, 11]) with $\gamma = (eF_0)^2/(8m^*\hbar\omega^3)$ being a dimensionless parameter. In equation (2), $J_m(x)$ is a Bessel function, $r_0 = eF_0/m^*\omega^2$ with a dimension of length, $V(Q) = 4\pi e^2/\kappa Q^2$ is the Fourier transform of the bare e–e interaction, and κ is the dielectric constant. Furthermore,

$$F_m(x) = \sum_{n=0}^{\infty} \frac{J_n(\gamma)}{1 + \delta_{n,0}} [J_{2n-m}(r_0 x) + (-1)^{m+n} J_{2n+m}(r_0 x)] \tag{3}$$

and

$$\Pi_0(\boldsymbol{Q}, \Omega) = \frac{g_s}{2\pi l^2} \sum_{N',N} C_{N',N}(l^2 q^2/2) \sum_{k_z} \frac{f(E_N(k_z) + E_{em}) - f(E_{N'}(k_z + q_z) + E_{em})}{\hbar\Omega + E_N(k_z) - E_{N'}(k_z + q_z) + \mathrm{i}\delta} \tag{4}$$

where $f(x)$ is the Fermi–Dirac function, $C_{N,N+J}(y) = [N!/(N + J)!]y^J \mathrm{e}^{-y}[L_N^J(y)]^2$ with $L_N^J(y)$ the associated Laguerre polynomial, and $E_N(k_z) = E_N + \hbar^2 k_z^2/2m^*$. The dielectric function given by equation (2) measures the strength of a gas of electrons interacting via their long-range force such as the Coulomb potential in the presence of the EM and magnetic fields. The non-perturbative theoretical approaches developed in this study have gone beyond the conventional many-body theory dealing with electron interactions with the radiation field in an electron gas system. In the results shown above, the effect of the radiation field is included exactly and multiphoton processes are also included. The detailed derivations of equations (1) and (2) were documented respectively in [7] and [9].

The magneto-plasmon modes induced by the charge–density excitation can be determined theoretically by the condition of the vanishing of the real part of the dielectric function, namely, by Re $\epsilon(\boldsymbol{Q}, \Omega) \to 0$. In the low-temperature (i.e. $T \to 0$) and long-wavelength (i.e. $Q \to 0$) limit, the frequency of the magneto-plasmon can be determined simply by

$$\Omega_{\pm}^2 = \tfrac{1}{2}[\omega_c^2 + \Omega_p^2 \pm \sqrt{(\omega_c^2 - \Omega_p^2)^2 + 4\Omega_p^2\omega_c^2 \sin^2\theta}] \tag{5}$$

where θ is the angle between the z-axis and the direction of plasmon propagation, and

$$\frac{\Omega_p^2}{\omega_p^2} = \frac{a}{\pi^2 l^2 N_e} \sum_N \Theta(E_F - E_N - E_{em})(E_F - E_N - E_{em})^{1/2} \tag{6}$$

with N_e being the electron density, E_F the Fermi energy and $\omega_p = (4\pi e^2 N_e/\kappa m^*)^{1/2}$ the plasmon frequency in the absence of the EM and magnetic fields.

In the presence of intense EM radiation and strong magnetic field, the electron DOS will be modified by the frequency ω and intensity F_0 of the radiation field and by the magnetic field (see (1)) and, consequently, the Fermi energy E_F is a function of ω and F_0 (see figure 1) and of B (see figure 2). Comparing equations (5) and (6) with those obtained in the absence of the EM field [6], we see that the influence of the laser radiation on magneto-plasmon excitations can occur via varying Ω_p given by (6). Noting that $E_F - E_N > E_{em}$ implies the presence of channels for optical absorption and elastic photon scattering for the Nth LL, the frequency Ω_p arises from electronic transitions via absorption of photons and via elastic photon scattering processes. For plasmon propagation parallel to the z-axis ($\theta = 0$),

$$\Omega_{\parallel,+} = \omega_c \qquad \text{and} \qquad \Omega_{\parallel,-} = \Omega_p. \tag{7}$$

For plasmon propagation perpendicular to the z-axis ($\theta = 90°$),

$$\Omega_{\perp,+} = \sqrt{\omega_c^2 + \Omega_p^2} \qquad \text{and} \qquad \Omega_{\perp,-} = 0. \tag{8}$$

Therefore, the effect of the laser radiation on magneto-plasmon excitations can be observed by measuring the dependence of $\Omega_{\parallel,-}$ and $\Omega_{\perp,+}$ on F_0 and ω (shown in figure 3) and on B (shown in figure 4). The numerical results presented in this letter are for a GaAs-based 3DEG system for which $m^* = 0.0665 m_e$ with m_e being the rest electron mass, $\kappa = 12.9$ and typically $N_e = 10^{17}$ cm^{-3}.

The results shown in figures 1 and 3 indicate the following.

(1) Under low-frequency and/or high-intensity radiations, when $E_{em} \gg \hbar\omega$, E_F is mainly determined by E_{em} via the dynamical Franz–Keldysh effect [10, 11]. E_{em} will result in a blue-shift of the energy spectrum of the electronic system. In this case: (i) $E_F - E_0 > E_{em}$; (ii) Ω_p, $\Omega_{\parallel,-}$ and $\Omega_{\perp,+}$ increase with increasing F_0 and/or decreasing ω and (iii) $\Omega_{\parallel,-} > \omega_p$ and $\Omega_{\perp,+} > \sqrt{\omega_c^2 + \omega_p^2}$ can be achieved.

(2) In an intermediate radiation frequency and intensity regime, E_F is determined mainly by photon emission processes. In this case: (i) $E_F - E_0 < E_{em}$ and $\Omega_p = 0$; (ii) $\Omega_{\perp,+} = \omega_c$ and (iii) $\Omega_{\parallel,-} = 0$, i.e. the excitation of this branch of the plasmon modes is suppressed.

(3) For relatively high-frequency and/or low-intensity radiations, E_F is determined mainly by the magnetic field and by 0-photon and photon absorption processes that result in $E_F - E_0 > E_{em}$. In this case Ω_p, $\Omega_{\parallel,-}$ and $\Omega_{\perp,+}$ increase with increasing ω and/or decreasing F_0 and $\Omega_{\parallel,-} < \omega_p$, $\Omega_{\perp,+} < \sqrt{\omega_c^2 + \omega_p^2}$.

(4) For $\omega \gg 1$ and/or $F_0 \ll 1$ so that $r_0 \to 0$ and $\gamma \to 0$, Ω_p tends to ω_p and, therefore, $\Omega_{\parallel,-} \sim \omega_p$ and $\Omega_{\perp,+} \sim \sqrt{\omega_c^2 + \omega_p^2}$. Since $\gamma \sim F_0^2/\omega^3$ and $r_0 \sim F_0/\omega^2$, the radiation frequency has a stronger effect on the collective excitations. The results shown above

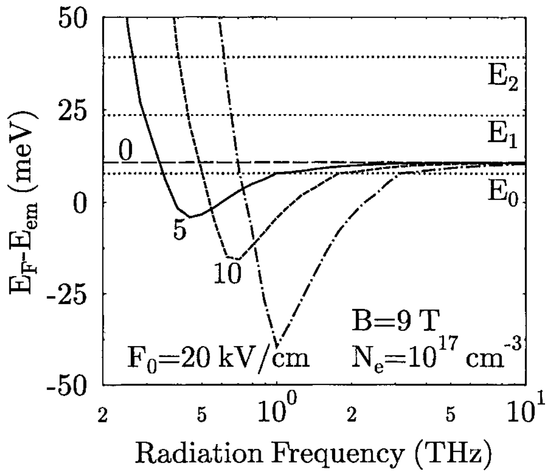

Figure 1. Fermi energy (E_F), measured from the energy of the radiation field (E_{em}), as a function of radiation frequency ($\omega/2\pi$) at a fixed magnetic field ($\boldsymbol{B}$) for different radiation intensities (F_0). E_N is the energy of the Nth LL and N_e is the electron density.

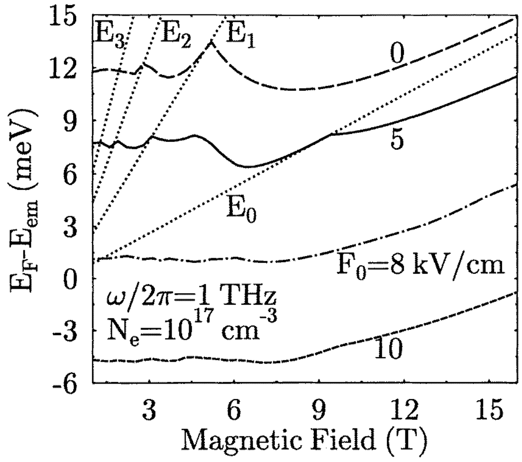

Figure 2. Fermi energy as a function of magnetic field at a fixed radiation frequency for different radiation intensities.

indicate that by altering the frequency and intensity of the THz laser field, tunable magneto-plasmon excitations can be achieved in a semiconductor system.

The dependence of the magneto-plasmon frequency on magnetic field is shown in figure 4 at a fixed radiation frequency for different radiation intensities. $F_0 = 0$ (dotted curves) corresponds to the situation where the radiation field is absent. From figure 2, we see that in the presence of intense laser radiation (e.g. $F_0 = 5$ kV cm^{-1} and $\omega/2\pi = 1$ THz), $E_F - E_0 - E_{em}$ decreases with increasing magnetic field. This is similar to the case in the absence of the EM field, where $E_F - E_0$ decreases with increasing $\boldsymbol{B}$, due to the deduction of electron density of states by the magnetic field. In high magnetic fields, the situation $E_F - E_0 < E_{em}$ can be achieved. As a consequence, as can be seen in figure 4, $\Omega_{\parallel,-} = 0$ and $\Omega_{\perp,+} = \omega_c$ can be observed at high

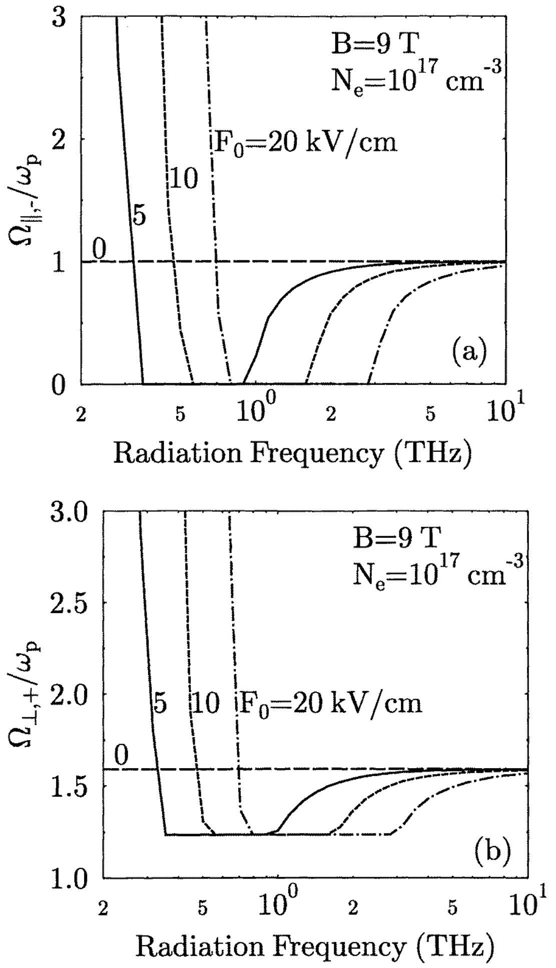

Figure 3. Magneto-plasmon frequency ($\Omega_{\|,-}$ in (a) and $\Omega_{\perp,+}$ in (b)) as a function of radiation frequency at a fixed magnetic field for different radiation intensities. ω_p is the plasmon frequency in the absence of the electromagnetic and magnetic fields. The signs $\|$ ($\perp$) refer to plasmon propagation parallel (perpendicular) to the z-direction along which the magnetic field is applied and the radiation field is polarized. The signs + and − correspond to different branches of the plasmon modes. For GaAs with $N_e = 10^{17}$ cm^{-3}, $\omega_p/2\pi = 3.07$ THz, and $\omega_c/2\pi = 3.80$ THz at $\boldsymbol{B} = 9$ T.

magnetic fields ($B > 10$ T) for $F_0 = 5$ kV cm^{-1} (full curves) and $\omega/2\pi = 1$ THz.

In the present study, the effect of phonon coupling on plasmon excitation is not taken into consideration. In order to include this effect within the calculations, one of the most tractable theoretical approaches is the ‘self-consistent field approximation’ (SCFA) [13]. However, the inclusion of the phonon scattering within the effective e–e interaction by using, e.g. the SCFA will complicate the analytical and numerical calculations considerably, especially to look into the problem in the time-representation. Therefore, I do not attempt it in the present study. Moreover, it can be expected that for magneto-plasmon excitation in the presence of laser radiation, the significant

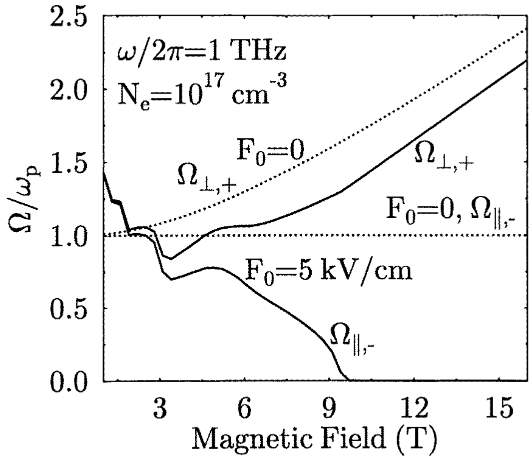

Figure 4. Magneto-plasmon frequency as a function of magnetic field at a fixed radiation frequency for different radiation intensities.

influence of the phonon scattering will occur at certain radiation and magnetic fields when the conditions such as magneto-phonon resonance (MPR) [14] and magneto-photon–phonon resonance (MPPR) [15] are satisfied. The results presented in this letter can be used to understand that the phenomena occurred away from these resonant conditions.

The investigation of collective excitations in semiconductor systems, such as plasmons, phonons, magnons and nuclear quanta, has played an important role in modern condensed matter physics and electronics. Experimentally, both far-infrared-absorption spectroscopy and inelastic-resonant-light-scattering spectroscopy have been used extensively to measure the plasmon spectra in semiconductor materials in the absence of intense laser radiation (for a review see [12]). So far, no experimental work on the effect of intense THz radiation on the plasmon spectrum in condensed matter materials has been reported.

For a GaAs-based electron gas driven by an EM field with $\omega/2\pi \sim 1$ THz and $F_0 \sim 10$ kV cm^{-1}, conditions such as $ar_0(E_F - E_N - E_{em} - m\overline{h}\omega)^{1/2} \sim 1$ and $\gamma \sim 1$ can be satisfied. As a consequence, the electronic structure and the electronic transitions can be affected strongly by the EM field and the spectrum of the magneto-plasmon can be modified by the frequency and intensity of the radiation. It should be noted that such radiation has been realized by the THz FEL sources developed recently in, e.g. UCSB (USA) [1] and FELIX (The Netherlands) [2]. Moreover, when a GaAs-based electron gas system is subjected to THz FEL radiation, the blue-shift of the energy spectrum by E_{em} the energy of the radiation field via the dynamical Franz–Keldysh effect has been successfully observed in a very recent experimental measurement [11]. I therefore hope that the phenomena discussed in this letter will be verified experimentally.

This work was supported by the Australian Research Council.

References

[1] Asmar N G, Markelz A G, Gwinn E G, Cerne J, Sherwin M S, Campman K L, Hopkins P F and Gossard A C 1995 *Phys. Rev.* B **51** 18 041

[2] Murdin B N, Heiss W, Langerak C J G M, Lee S-C, Galbraith I, Strasser G, Gornik E, Helm M and Oidgeon C R 1997 *Phys. Rev.* B **55** 5171
[3] Xu W and Zhang C 1996 *Appl. Phys. Lett.* **68** 829
[4] Xu W 1998 *J. Phys.: Condens. Matter* **10** 10 787
[5] Koenraad P M, Lewis R A, Waumans L R C, Langerak C J G M, Xu W and Wolter J H 1998 *Proc. 24th Int. Conf. on Phys. Semicond.* (Singapore: World Scientific) at press
[6] See, e.g., Mermin N D and Canel E 1964 *Ann. Phys.* **26** 247
[7] Xu W 1997 *J. Phys.: Condens. Matter* **9** L591
[8] See, e.g., Mattuck R D 1976 *A Guide to Feynman Diagrams in the Many-Body Problem* (New York: McGraw-Hill)
[9] Xu W 1999 *Phys. Rev.* B **59** 10 869
[10] Jauho A P and Johnsen K 1996 *Phys. Rev. Lett.* **76** 4576
[11] Nordstrom K B, Johnsen K, Allen S J, Jauho A-P, Birnir B, Kono J, Noda T, Akiyama H and Sakaki H 1998 *Phys. Rev. Lett.* **81** 457
[12] Pinczuk A and Abstreiter G 1989 *Light Scattering in Solids V* ed M Cardona and G Guntherodt (Berlin: Springer)
[13] Mahan G D 1981 *Many-Particle Physics* (New York: Plenum)
[14] Leadley D R *et al* 1994 *Phys. Rev. Lett.* **73** 589
[15] Xu W and Zhang C 1996 *Phys. Rev.* B **54** 4907